APPLYING SYMMETRICAL COMPONENT TRANSFORM FOR INDUSTRIAL APPLIANCE CLASSIFICATION IN NON-INTRUSIVE LOAD MONITORING

Anthony Faustine [*]*, Lucas Pereira*

ITI, LARSyS, Técnico Lisboa, Lisbon, Portugal

ABSTRACT

Industrial loads offer challenges for Non-intrusive Load Monitoring (NILM), such as phase imbalance associated with 3-phase lines. However, very little NILM research has been developed so far with this respect. This work presents a load recognition technique for NILM applying low complexity Fortesque Transform (FT). The FT decomposes the unbalanced 3-phase current waveform extracted from 3-phase aggregate power measurements to balance the given load. The 3-phases current waveform is transformed into an image-like representation using a compressed-euclidean distance matrix to improve the recognition ability further. The image representation is used as input to Convolutional Neural Network (CNN) classifier to learn the patterns of labeled data. Experimental evaluation of the industrial aggregated dataset shows that FT improves recognition performance by 5.8%, compared to the case without FT.

***Index Terms*—** NILM, Industrial Appliances, Three-Phase, Fortesque Transform, Symmetrical Components

1. INTRODUCTION

The rise in industrial energy use is of great concern to climate and sustainability challenges and currently accounts for 40% of global Greenhouse Gas (GHG) emissions. Hence, understanding the consumption profiles of individual industrial machinery can play an essential role in designing customized energy efficiency and demand management strategies in the industrial sector [1, 2, 3].

Non-Intrusive Load Monitoring (NILM) is a computation technique that extracts appliance-specific energy consumption profiles from aggregate consumption data monitored at the mains [4]. A critical step in NILM pipelines is to identify and extract features that are distinctive enough to discriminate across different appliances. In this regard, several approaches have been proposed for residential appliances, with high-frequency current-voltage(V-I) waveforms-based features consistently achieving state-of-the-art performances [5, 6, 7, 8, 9, 10, 11, 12].

[*]Anthony Faustine work at Center of Intelligent Power (CIP), Eaton Dublin

Identifying unique and distinct features can be challenging in an industrial setting with a three-phase power system owing to phase imbalance. In fact, industrial environments often consist of three-phase machines equipped with various equipment such as larger motors and drives [13]. It is also likely to find single-phase appliances that will lead to phase imbalance, as well as the combination of single- and three-phase machines with extensive energy consumption ranges that will make extracting distinctive features for appliance recognition very challenging. The phase imbalance will likely affect the feature extraction stage of the event-based NILM, especially when the small-consuming appliance has proceeded with larger motors, as illustrated in Figure 1.

There is limited research about using NILM to disaggregate industrial machinery [13], and phase imbalance was not considered in the few existing works. The work in [14] demonstrates a neural-net-based NILM algorithm for energy disaggregation of a chiller plant system in a commercial building for energy monitoring purposes. In [2], the authors present the FHMM NILM algorithm for energy disaggregation of machinery in a brick production factory. An optimization algorithm for NILM in three different industrial sectors: food processing, stonecutting, and glassmaking, is presented in [15]. Finally, the work presented in [16] demonstrates that transforming the current waveform into an image-like representation using compressed distance and feeding it as input to a Convolutional Neural Network (CNN) offers higher appliance recognition performance in a three-phase system that included industrial loads. Yet, the presented approaches did not exploit the phase imbalance common in an industrial setting.

This work exploits the multi-dimension nature of the unbalanced three-phase system in an industrial setting through low-complexity Fortesque Transform (FT). FT is an instantaneous symmetrical component [17], a well-known tool for calculating power quality in electrical grids [18]. It has been applied to various problems such as fault location and recognition [19, 17] and in generating the reference currents for the converters in micro-grid systems [20].

More precisely, the FT decomposes the unbalanced three-phase current into a set of three components to balance the given load. The base assumption is that decomposing the three-phase current will help extract distinctive current fea-

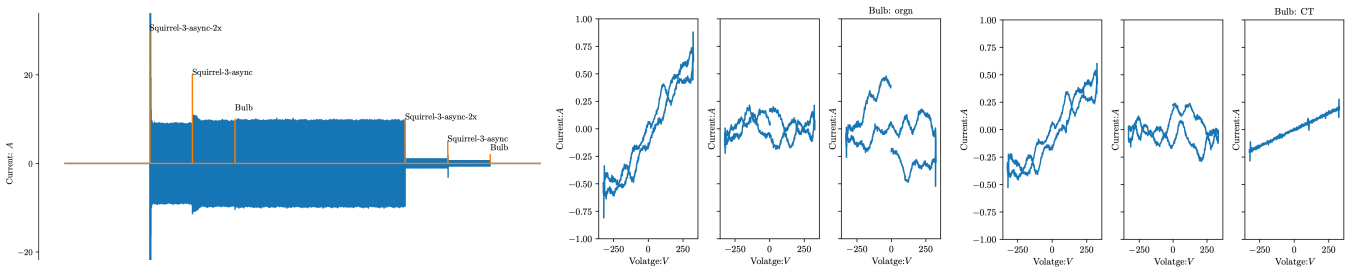

(a) Current waveform for different events

(b) V-I with phase imbalance

(c) V-I after FT

Fig. 1. Impact of a three-phase load on the activation of a single-phase appliance: a) current waveform for different events, b) The distorted current-voltage trajectory of a bulb activation caused by the influence of a large three-phase load, c) The restored current-voltage activation of a bulb following the application of Fourier Transform (FT).

tures, especially when a small-single phase appliance is preceded by a large three-phase load, as illustrated in Figure 1. For appliance recognition, we follow [16] and transform the balanced 3-phase current waveform into an image-like representation using a compressed-euclidean distance matrix, which is input to the CNN classifier.

2. PROPOSED METHODS

A three-phase electrical system widely used in industrial environment consist set of three voltages and currents. In time-domain, the unbalanced three-line voltages, and currents can be expressed as:

$$s_1(t) = a_1(t)\cos(2\pi f_0 t + \phi) + \eta_1(t) \quad (1)$$

$$s_2(t) = a_2(t)\cos(2\pi f_0 t + \phi - \frac{2\pi}{3}) + \eta_2(t) \quad (2)$$

$$s_3(t) = a_3(t)\cos(2\pi f_0 t + \phi + \frac{2\pi}{3}) + \eta_3(t) \quad (3)$$

Where:

- $s_k(t)$ represents the AC signal, either voltage or current,
- $a_k(t)$ is the amplitude of the signal around the fundamental frequency f_0,
- ϕ is the original phase shift of $s_1(t)$, and
- $\eta_k(t)$ is the additive noise present in the signal $s_k(t)$

In an ideal situation, the three-phase system is assumed to be balanced such that the three quantities have the same amplitude ($a_1(t) = a_2(t) = a_3(t)$) and an equal phase shift of $\frac{2\pi}{3}$. However, in industrial setting the balance assumption usually does not hold. As the result, a symmetrical component transform such as FT will decompose the unbalanced three-phase system into balanced and unbalanced components, namely positive, negative and zero-sequence components [21].

Given a three-phase signal $\mathbf{S}(t) = [s_1(t), s_2(t), s_3(t)]^T$, the transformed FT components $\mathbf{S}_{+,-,0}$ are given by

$$\mathbf{S}_{+,-,0} = \begin{bmatrix} s_+(t) \\ s_-(t) \\ s_0(t) \end{bmatrix} = \frac{2}{3}\mathbf{F}\mathbf{s}(t) \quad (4)$$

where:

$$\mathbf{F} = \begin{bmatrix} 1 & a & a^2 \\ 1 & a^2 & a \\ 1 & 1 & 1 \end{bmatrix} \quad (5)$$

where $a = e^{j\frac{2}{3}}$.

For balanced three-phase systems, only the $s_+(t)$ and $s_-(t)$ sequence exists, while the zero-sequence $s_0(t)$ will be null. Thus, the zero-sequence $s_0(t)$ can quantify the amount of imbalance in the three-phase signal. We utilize this hypothesis and assume that the zero component $s_0(t)$ will represent the appliance signature of a single-phase appliance in case of phase imbalance as shown in Figure 1c.

2.1. Feature Extraction and Pre-Processing from Aggregate Measurements

We consider appliance features extracted in brief time windows to recognize appliances containing only one event feature derived from three-phase aggregate power measurements. Thus an activation current i and voltage v is obtained by first measuring 25 complete cycles of current and voltage before $\{\mathbf{i}_k^{(b)}, \mathbf{v}_k^{(b)}\}$ and after $\{\mathbf{i}_k^{(a)}, \mathbf{v}_k^{(a)}\}$ the event, where $k \in \{1, 2, 3\}$. The 25 cycles correspond to steady-state behavior and are equivalent to $T_s \times N_s$ samples where $T_s = \frac{f_s}{f}$, $f_s = 50KHz$ is the sampling frequency, and $f = 100Hz$ is the mains frequency. We aligned the 25 extracted cycles at the zero-crossing of the voltage and then applied an FT to decompose them into three components such that:

$$\mathbf{i}_{+,-,0}^{(b)} = \frac{2}{3}\mathbf{F}\mathbf{i}^{(b)} \quad (6)$$

$$\mathbf{i}_{+,-,0}^{(a)} = \frac{2}{3}\mathbf{F}\mathbf{i}^{(a)} \quad (7)$$

The procedure for determining the one-cycle activation current and voltage for an appliance involves obtaining the difference between the current values before and after an event [16].

2.2. Compressed Euclidean Distance Matrix

The Euclidean Distance Matrix (EDM) is the matrix of squared Euclidean distances representing the spacing of a set of w points in euclidean space [22] such that:

$$D_{w,w} = \begin{bmatrix} 0 & d_{1,2} & \cdots & d_{1,w} \\ d_{2,1} & 0 & \cdots & d_{2,w} \\ \vdots & \vdots & \ddots & \vdots \\ d_{w,1} & d_{w,2} & \cdots & 0 \end{bmatrix} \tag{8}$$

where $d_{u,v} = ||i(t)_u - i(t)_v||_2$ is the Euclidean distance function which is widely used as a pre-processing step for many machine learning approaches such as K-means clustering and K-nearest neighbor algorithms [23, 22]. The compressed EDM provides a relationship metric between each element in the time series. It encodes time series data into a recurrence graph (RP) which reveals at which point trajectories return to a previous state. It is usually formulated such that:

$$RG_{i,j} = \begin{cases} \delta & \text{if} \quad \tau > \delta \\ \tau & \text{otherwise} \end{cases} \tag{9}$$

where $\tau = \left\lfloor \frac{d_{u,v}}{\epsilon} \right\rfloor$, $0 < \epsilon \leq 1$ and $\delta \geq 1$

Thus to generate RG images of size $w \times w$, the piecewise aggregation approximation (PAA) [24, 1], is first applied to reduce the signal's dimension from T_s to a predefined size w with minimal information loss. The embedding size w is the hyper-parameter that needs to be selected in advance. Previous works confirmed that the choice of w does not significantly influence the classification performance. Yet, large values of w impact the learning speed, and very small values of w will most likely lead to larger information loss [1, 16]. The PAA signal is then transformed into an RP image using Equation (9).

2.3. Classifier and Training Procedure

A 2-stage CNN is used to learn the appliance labels. Each CNN layer contains 50 feature maps with a filter size of 5×5, stride size of 1×1, and ReLU activation function followed by a pooling layer with a filter size of 2×2. The final layer consists of two FC layers with a hidden dimension of w^2 and K, respectively, where K is the number of classes determined by the number of appliances available. The final predicted class is obtained by applying the softmax activation function. Since the problem at hand is the multi-class classification, and the Cross-Entropy Loss function defined in Equation (10) is used.

$$\mathcal{L}_\theta(y, p) = -\sum_{i=1}^{M} y_i \cdot \log p_i \tag{10}$$

The CNN network is trained for 600 iterations using mini-batch Stochastic Gradient Descent (SDG) with a momentum of 0.9, a learning rate of 1^{-3}, and a batch size of 16. To avoid over-fitting, early stopping with patience is used where the training model is terminated once the validation performance does not change after 20 iterations.

2.4. Evaluation Procedure

The proposed method is evaluated on the Laboratory-measured Industrial Load of Appliance Characteristics dataset (LILACD) [25]. The dataset contains three-phase aggregated and sub-metered current and voltage measurements sampled at 50 kHz for 16 different appliance types (industrial and home appliances). In this study, aggregated measurement data that contain measurements of more than one concurrently running appliance is used. Since the dataset is multi-dimensional, a separate activation current for each current phase is an input feature.

We adopt stratified 4-fold cross-validation with a random shuffle to benchmark our approach. The 4-fold cross-validation with a random shuffle provides stratified randomized folds while preserving the label's percentage in each fold. We analyzed the FT influence by assessing the recognition appliance performance with and without FT transform. This was achieved by training the CNN-based classifier with RG and V-I feature representation. The V-I was generated using the same process for generating binary V-I described in [7, 1].

We quantitatively evaluate the classification performance with macro averaged F_1 (%) score is defined as $F_{macro} = 100 \cdot \frac{1}{M} \sum_{i=1}^{M} F_1^{(i)}$ where M is the number of appliances and F_1 is the harmonic mean of precision and recall. We also use the confusion matrix, which shows the correct predictions (the diagonal) and provides a clear view of which appliances are confused with each other. The following abbreviations are utilized: Compact fluorescent lamp (CFL), Bulb (ILB), Kettle (KT), Coffee Maker (CM), Hair-dryer (HD), Raclette (RC), and FridgeDefroster (FRZ), 1-phase-async-motor (1P-Motor), and Drilling machine (DRL) for single phase appliances. The three-phase industrial appliances include Dumper-machine (3P-DPM), 2x=Freq-conv-squirrel-3-2x (3P-FCS), Squirrel-3-async (3P-SQL), and Squirrel-3-async-2x(3P-SQL-2x).

3. RESULTS AND DISCUSSION

Figure 2 presents the per-appliance F-score for the two feature representations with and without FT transform. In both cases,

we see that the RP achieves a high F-score compared to V-I. We also see that when FT is used, the RP performs overall 96.43 scores compared to 94.21 when FT is not applied. We further see in Figure 2b that the RP with FT attains an F-score above 0.9 for all appliances. Notably, the V-I achieve a low score of less than 60 for single-phase appliances such as Coffe-machine, Kettle, Raclette, and Hairdryer.

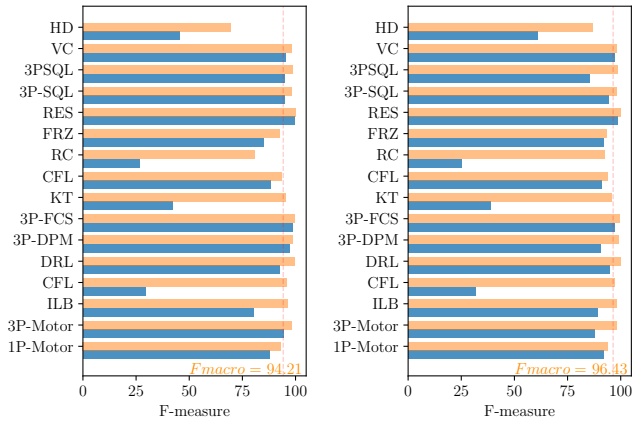

(a) Without FT (b) RP with FT

Fig. 2. Classification Results: a) F-score combined phases without FT for VI and RP b) F-score combined phases with FT for VI and RP.

Investigating the confusion matrix in Figure 3, we observe that the RP without FT makes several confusions between Hair-dryer and Raclette. We also see that applying FT improves the recognition performance of most single-phase appliances. The results suggest that the proposed FT transform can improve the process of extracting appliance signatures that is distinct enough to recognize appliances especially when there is a phase imbalance, as initially hypothesized.

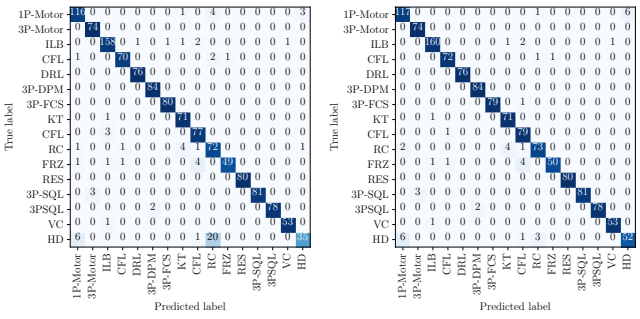

(a) Without FT (b) RP with FT

Fig. 3. Confusion matrix: a) RP without FT, b) RP with FT.

4. CONCLUSION

In this work, we have applied low-complexity Fortesque Transform to improve the discrimination power of NILM for industrial machinery recognition. The FT decomposes the unbalanced three-phase current waveform into a set of three components to balance the given load. The decomposed current signal was then transformed into an image-like representation using the euclidean-distance-similarity function (RG) and fed into the CNN for classification.

We then present the outcome of an empirical investigation on how FT influences the classification performance for RP and V-I features. We observe that applying FT improves classification performances for both V-I and RP features. The outcomes further suggest that the RP feature with FT is consistently superior to those from V-I images with FT. Most importantly, RP with FT can identify single-phase appliances whose signatures have been distorted by phase imbalance and high-consuming appliances. Ultimately, these results suggest that industries could effectively use the proposed approach to disaggregate industrial machinery and allow value-added services such as predictive maintenance by monitoring power consumption from a single point source.

Finally, while the results argue in favor of the proposed approach, it is important to acknowledge that the experimental procedure is limited to one single dataset. Hence, to better generalize the findings, further experimentation is required in other datasets. Furthermore, it is important to remark that the developed method assumes perfect detection of the appliance change of state (i.e., from ON to OFF and vice-versa), which may be hard to achieve especially in an industrial setting where the aggregated signal tends to be far more complex than for example in residential spaces. Therefore, future work iterations should also consider the effect of appliance state change detection in the overall non-intrusive appliance identification process.

Acknowledgement

Lucas Pereira received funding from FCT under grants CEECIND/01179/2017, and UIDB/50009/2020.

5. REFERENCES

[1] Anthony Faustine and Lucas Pereira, "Improved appliance classification in non-intrusive load monitoring using weighted recurrence graph and convolutional neural networks," *Energies*, vol. 13, no. 13, pp. 3374, July 2020.

[2] Fan Yang, Bo Liu, Wenpeng Luan, Bochao Zhao, Zishuai Liu, Xiao Xiao, and Ruiqi Zhang, "Fhmm based industrial load disaggregation," in *2021 6th Asia Con-*

ference on Power and Electrical Engineering (ACPEE), 2021, pp. 330–334.

[3] Miguel Angel Bermeo-Ayerbe, Carlos Ocampo-Martinez, and Javier Diaz-Rozo, "Data-driven energy prediction modeling for both energy efficiency and maintenance in smart manufacturing systems," *Energy*, vol. 238, pp. 121691, 2022.

[4] G.W. Hart, "Nonintrusive appliance load monitoring.," *Proceedings of the IEEE*, vol. 80, no. 12, pp. 1870–1891, 1992.

[5] L. Du, D. He, R. G. Harley, and T. G. Habetler, "Electric load classification by binary voltage–current trajectory mapping," *IEEE Transactions on Smart Grid*, vol. 7, no. 1, pp. 358–365, Jan 2016.

[6] J. Gao, E. C. Kara, S. Giri, and M. Bergés, "A feasibility study of automated plug-load identification from high-frequency measurements," in *2015 IEEE Global Conference on Signal and Information Processing (GlobalSIP)*, Dec 2015, pp. 220–224.

[7] Leen De Baets, Joeri Ruyssinck, Chris Develder, Tom Dhaene, and Dirk Deschrijver, "Appliance classification using vi trajectories and convolutional neural networks," *ENERGY AND BUILDINGS*, vol. 158, pp. 32–36, 2018.

[8] L. De Baets, T. Dhaene, D. Deschrijver, C. Develder, and M. Berges, "Vi-based appliance classification using aggregated power consumption data," in *2018 IEEE International Conference on Smart Computing (SMARTCOMP)*, June 2018, pp. 179–186.

[9] Y. Liu, X. Wang, and W. You, "Non-intrusive load monitoring by voltage–current trajectory enabled transfer learning," *IEEE Transactions on Smart Grid*, vol. 10, no. 5, pp. 5609–5619, Sep. 2019.

[10] Darío Baptista, Sheikh Mostafa, Lucas Pereira, Leonel Sousa, and Dias F. Morgado, "Implementation strategy of convolution neural networks on field programmable gate arrays for appliance classification using the voltage and current (v-i) trajectory," *Energies*, vol. 11, pp. 2460, 09/2016 2018.

[11] A. Longjun Wang, B. Xiaomin Chen, C. Gang Wang, and D. Hua, "Non-intrusive load monitoring algorithm based on features of v–i trajectory," *Electric Power Systems Research*, vol. 157, pp. 134 – 144, 2018.

[12] Karim Said Barsim, Lukas Mauch, and Bin Yang, "Neural Network Ensembles to Real-time Identification of Plug-level Appliance Measurements," in *Proceeding of the 2016 NILM workshop*, 2016.

[13] Simon Henriet, Umut Şimşekli, Benoit Fuentes, and Gaël Richard, "A generative model for non-intrusive load monitoring in commercial buildings," *Energy and Buildings*, vol. 177, pp. 268 – 278, 2018.

[14] Benjamin Si Hao Chew, Yan Xu, and Ding Hong Yuan, "Non intrusive load monitoring for industrial chiller plant system - a long short term memory approach," in *2019 9th International Conference on Power and Energy Systems (ICPES)*, 2019, pp. 1–5.

[15] Sara Tavakoli and Kaveh Khalilpour, "A practical load disaggregation approach for monitoring industrial users demand with limited data availability," *Energies*, vol. 14, no. 16, 2021.

[16] A. Faustine, L. Pereira, and C. Klemenjak, "Adaptive weighted recurrence graphs for appliance recognition in non-intrusive load monitoring," *IEEE Transactions on Smart Grid*, pp. 1–1, 2020.

[17] D. I. Ivanchenko and B. A. Aleksey, "Transformer fault analysis using instantaneous symmetrical components," in *2018 IEEE Conference of Russian Young Researchers in Electrical and Electronic Engineering (EIConRus)*, 2018, pp. 641–644.

[18] J. Suma and M. K. Mishra, "Instantaneous symmetrical component theory based algorithm for characterization of three phase distorted and unbalanced voltage sags," in *2013 IEEE International Conference on Industrial Technology (ICIT)*, 2013, pp. 845–850.

[19] X. F. St-Onge, J. Cameron, S. Saleh, and E. J. Scheme, "A symmetrical component feature extraction method for fault detection in induction machines," *IEEE Transactions on Industrial Electronics*, vol. 66, no. 9, pp. 7281–7289, 2019.

[20] N. R. Tummuru, M. K. Mishra, and S. Srinivas, "Multifunctional vsc controlled microgrid using instantaneous symmetrical components theory," *IEEE Transactions on Sustainable Energy*, vol. 5, no. 1, pp. 313–322, 2014.

[21] Gianfranco Chicco and Andrea Mazza, "100 years of symmetrical components," *Energies*, vol. 12, no. 3, 2019.

[22] I. Dokmanic, R. Parhizkar, J. Ranieri, and M. Vetterli, "Euclidean distance matrices: Essential theory, algorithms, and applications," *IEEE Signal Processing Magazine*, vol. 32, no. 6, pp. 12–30, 2015.

[23] Santiago Ontañón, "An overview of distance and similarity functions for structured data," *Artificial Intelligence Review*, Feb. 2020.

[24] Eamonn J. Keogh and Michael J. Pazzani, "Scaling up dynamic time warping for datamining applications," in *Proceedings of the Sixth ACM SIGKDD International Conference on Knowledge Discovery and Data Mining*, New York, NY, USA, 2000, KDD '00, pp. 285–289, ACM.

[25] Matthias Kahl, Veronika Krause, Rudolph Hackenberg, Anwar Ul Haq, Anton Horn, Hans-Arno Jacobsen, Thomas Kriechbaumer, Michael Petzenhauser, Mikhail Shamonin, Anton Udalzow, and et al., "Measurement system and dataset for in-depth analysis of appliance energy consumption in industrial environment," *tm - Technisches Messen*, vol. 86, no. 1, pp. 1–13, 2019.